Catalyst Deactivation Modes in Nickel-Catalyzed Suzuki–Miyaura Cross-Coupling Reactions Using an NHC-Pyridonate Ligand

Abhishek A. Kadam, Medina Afandiyeva, William W. Brennessel, and C. Rose Kennedy

Department of Chemistry, University of Rochester, Rochester, NY 14627, USA

Supporting Information Placeholder

ABSTRACT: The catalytic activity of an NHC-pyridonate-supported nickel(0) complex for Suzuki–Miyaura coupling of aryl halides was evaluated. Product formation was observed in the absence of a basic additive. However, low turnover numbers resulted from competitive catalyst deactivation. The nature of catalyst deactivation—dimerization of the nickel(II) aryl intermediate—was elucidated through a combination of NMR monitoring, direct synthesis, and X-ray diffraction. This discovery was leveraged to identify additives that enable improved catalyst stability and turnover, thereby highlighting both the promise and pitfalls associated with incorporating secondary-sphere modifications for cooperative catalysis.

Suzuki–Miyaura cross-coupling reactions between (typically) aryl halide electrophiles and an organoboron nucleophiles have become among the most widely adopted synthetic transformations in fields spanning medicinal chemistry, agrochemical manufacturing, and synthesis of organic electronic materials.[1-8] The utility of this transformation stems from the bench-stability and ease-of-handling typical for boronic acid nucleophiles along with the reliability of highly optimized palladium catalyst systems, informed by decades of mechanistic study.[9-12] Despite these appealing features, there is substantial interest in the development of alternative catalytic methods, using more terrestrially-abundant metals such as nickel.[13, 14] Notwithstanding promising successes, there remain substantial challenges to the development of nickel-catalyzed Suzuki-Miyaura cross-coupling reactions that rival their palladium-catalyzed counterparts.[13, 15-17] One of such limitation is the comparatively unfavorable transmetallation of organoboron nucleophiles to nickel vs. palladium (Scheme 1A).[18-20] This arises, in part, due to the lower electronegativity of nickel ($\chi_P = 1.91$) compared to palladium ($\chi_P = 2.20$) and boron ($\chi_P = 2.04$), thereby necessitating strong activators to modulate the relative electronegativities of the metal and metalloid.[21, 22]

Our group previously reported NHC-pyridonate-supported nickel complexes that enable secondary-sphere activation of HBpin (4,4,5,5-tetramethyl-1,3,2-dioxaborolane) for hydroboration of alkenes and nitriles (Scheme 1B).[23, 24] NHC ligands are frequently employed in a variety of nickel-catalyzed cross-coupling reactions.[16, 25-27] Accordingly, we envisioned a similar activation mode may be accessible for organoboron reagents in the context of Suzuki–Miyaura coupling, wherein association of the pyridonate oxygen and Lewis acidic organoboron reagent in the secondary-coordination-sphere would simultaneously modulate the relative electronegativities of both transmetallation partners and provide further rate-acceleration through induced intramolecularity (Scheme 1C). In principle, this approach could obviate the need for a basic hydroxide or alkoxide activator.[19, 20] During our studies, a conceptually similar strategy using a phosphine ligand bearing a tethered alcohol was reported by Diao and coworkers.[28]

Scheme 1. Context and design strategy for Suzuki-Miyaura cross coupling using NHC-pyrdinate-supported nickel.

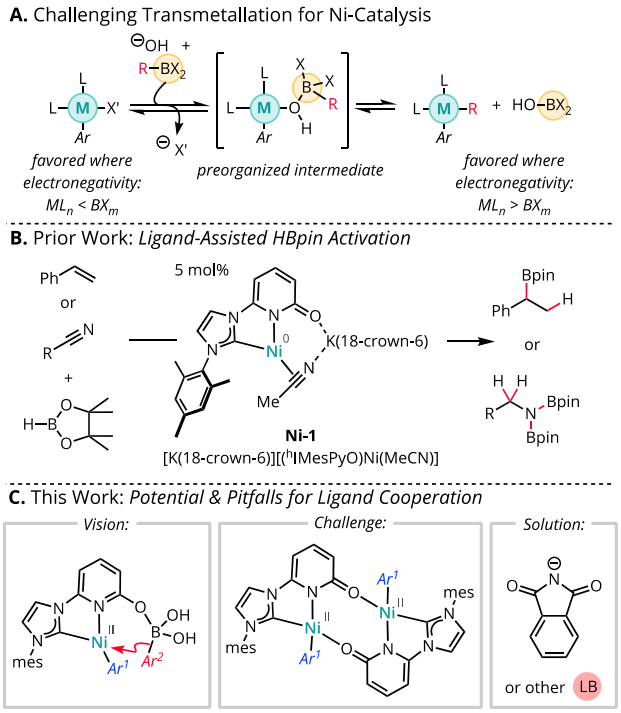

Herein we describe efforts toward the development of a nickel-catalyzed Suzuki–Miyaura cross-coupling reaction utilizing an NHC-pyridonate ligand to support secondary-coordination-sphere nucleophile activation (Scheme 1C). Through the combination of catalytic screening, NMR monitoring, direct synthesis, and structure elucidation through single-crystal X-ray diffraction (SC-XRD) analysis, these studies expose a unique mechanism for catalyst deactivation in

the presence of aryl halide substrates. Hypothesis-driven strategies are described to overcome this limitation through judicious choice of additives. This work thus highlights both the promise and pitfalls associated with leveraging secondary-sphere modifications for catalysis.

For evaluation of Suzuki–Miyaura cross-coupling catalysis, we selected 4-fluoroiodobenzene (**1**) and 4-(methoxy)phenylboronic acid (**2**) as model substrates, due to their diagnostic ^{19}F and ^{1}H NMR signatures. An initial survey of reaction conditions is summarized in Scheme 2.

Scheme 2. Initial survey of catalytic activity in a model Suzuki–Miyaura cross coupling reaction.

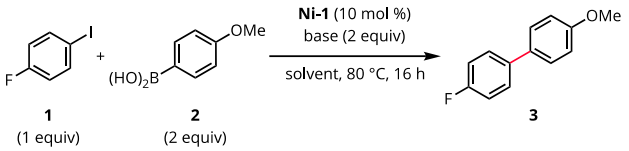

1 (1 equiv) **2** (2 equiv) **3**

Entry	Base	Solvent	Conv. of **1** [a]	Yield of **3** (TON) [b]
1	none	THF	23%	6% (<1)
2	none	NMP	34%	3% (<1)
3	KF	THF	32%	8% (<1)
3	KF	NMP	26%	3% (<1)
4	Na_2CO_3	THF	29%	6% (<1)
5	K_3PO_4	THF	31%	5% (<1)
6	KO^{t}Bu	THF	>99%	5% (<1)
7	KO^{t}Bu	NMP	>99%	3% (<1)
8	KO^{t}Bu	PhMe	>99%	trace

[a] Determined by GC from integration relative to dodecane as an internal standard. [b] Based on ^{1}H and ^{19}F NMR integration of diagnostic resonances relative to dodecane and fluorobenzene as internal standards.

Using the anionic precatalyst [K(18-crown-6)][(^{h}IMesPyO)Ni(MeCN)] (**Ni-1**) (10 mol%) in either the absence or presence of base afforded biaryl **3** in 3–8% yield after 16 hours at 80 °C in THF. Neither the inclusion nor identity of base had a substantive impact on the overall yield of cross-coupled product **3**. However, use of KO^{t}Bu as base resulted in substantially increased levels of both electrophile and nucleophile homocoupling (see Supporting Information). While arene solvent (toluene) inhibited reactivity, presumably due to low solubility, other Lewis basic solvents (e.g. NMP) performed similarly to THF.

The non-zero product yield in the presence of **Ni-1** and absence of base indicates that (i) an exogenous activator is not necessary to achieve transmetallation of boronic acid **2**, and (ii) the active complex is capable of productive C–C bond formation. However, the low turnover numbers (TON<1) suggests that some deactivation process limits regeneration of the active catalyst. We recognized that this deactivation process could result either (i) from failure to regenerate the active complex in the first catalytic turnover; or (ii) from a competitive mechanism for catalyst death at another point along the catalytic cycle.

We envisioned that monitoring the fate of **Ni-1** and electrophile **1** by ^{1}H and ^{19}F NMR spectroscopy would prove informative in evaluating these possibilities. However, upon treating **Ni-1** with electrophile **1** (1 equiv) in benzene-d_6 or toluene, the resulting product precipitated from solution, precluding further analysis. Following a survey of routinely available deuterated solvents, methanol-d_4 was identified as affording the highest quality spectra (balancing solubility, stability, and cost) for both **Ni-1** and its resulting products. Upon resuspending the crude precipitate in methanol-d_4, ^{1}H and ^{19}F NMR spectroscopic features were found to be consistent with a single major (^{19}F NMR δ: –125.6 ppm) and three minor (^{19}F NMR δ: –117.0, –118.3, and –125.7 ppm) fluorophenyl-containing products (Scheme 3). Upon the addition of boronic acid **2** and heating to 80 °C for 4 hours, the three minor species were largely consumed, as evidenced by the disappearance or decreased magnitude of the ^{19}F NMR resonances at –117.0, –118.3, and –125.7 ppm, coincident with the appearance of a new signature at –115.6 ppm (corresponding to product **3**). However, the resonance at –125.6 ppm persisted, even after heating to 80 °C for 24 hours. These observations suggested that understanding the structure and identity of this major component would be crucial for understanding catalyst deactivation.

Scheme 3. ^{19}F NMR monitoring of nickel speciation.

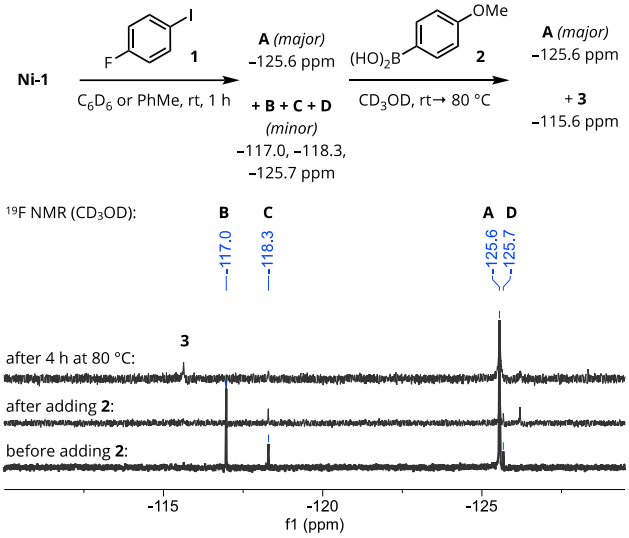

Purification and complete structural elucidation of the products derived from electrophile **1** proved challenging. We therefore elected to use 2-iodotoluene (**5a**) and 2-bromotoluene (**5b**) as model electrophiles for isolation experiments due to the precedent for *ortho*-substitution stabilizing otherwise challenging-to-isolate Ni(II) aryl complexes.[29-33] To enable comparison, a series of experiments were performed in which excess 2-halotoluene (**5a** or **5b**) was added to a solution of either anionic **Ni-1** or neutral analog **Ni-2** at ambient temperature.[34] In each case, a color change from purple to crimson red or orange was observed within 1–2 hours. The resulting suspensions were concentrated in vacuo and washed with pentane and diethyl ether prior to analysis by ^{1}H NMR spectroscopy and recrystallization from THF to afford crystals suitable for SC-XRD.

As expected, neutral **Ni-2** reacted with 2-iodotoluene (**4a**) or 2-bromotoluene (**4b**) to afford the classical oxidative addition products, [(^{h}IMesPy)NiX(*o*-tol)] where X = I (**Ni-3I**) or Br (**Ni-3Br**) (Scheme 4A).[35] The solid-state coordinates further revealed exclusive formation of the isomer with the electron-rich, σ-donating aryl ligand *trans* to the π-accepting pyridine. By contrast, the reaction of anionic **Ni-1** with either 2-iodotoluene (**4a**) or 2-bromotoluene (**4b**) in C_6H_6 afforded the

same diamagnetic product in both cases (Scheme 4B). The analogous reaction with 2-chlorotoluene (**4c**) required extended time and elevated temperature (50 °C, overnight) but also afforded the same diamagnetic product. Single-crystal X-ray diffraction (SC-XRD) analysis revealed the structure of neutral, dimeric Ni(II) aryl complex **[Ni-5]**$_2$. Presumably, this dimeric adduct formed following oxidative addition and dissociation of the halide ligand to afford three-coordinate Ni(II) complex **Ni-5**. In the absence of an alternative neutral ligand, the pyridonate acted as a 1,3-bridging ligand.

Scheme 4. Oxidative addition reactivity of NHC-pyridine and NHC-pyridonate-supported Ni complexes.

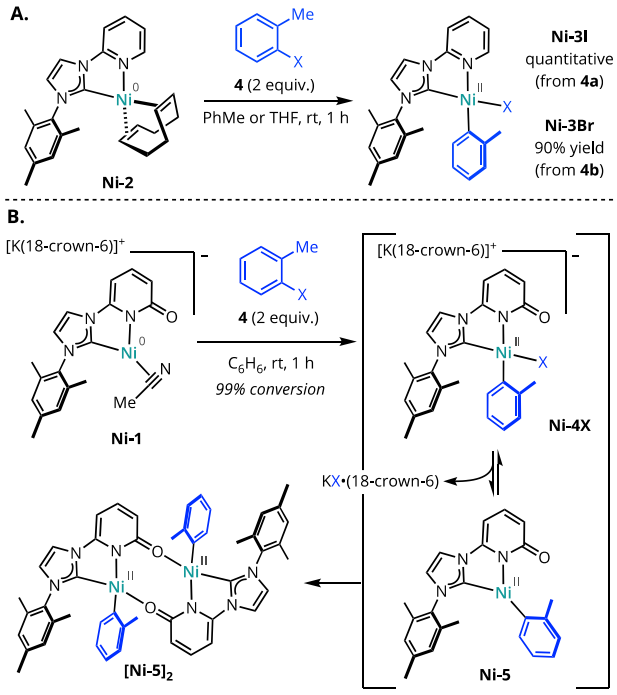

The solid-state structures and key bonding metrics for **Ni-3I**, **Ni-3Br**, and **[Ni-5]**$_2$ are shown in Figure 1 and Table 1. Most notably, the (pyridonate)N–Ni and (pyridonate)O–Ni bond lengths were found to be 1.97 and 1.92 Å, and the bond length of pyridonate C–O bond was found to be 1.28 Å, suggesting double-bond character. Taken together with the alternating bond lengths of the pyridonate backbone, these metrics are most consistent with the pyridonate ligand serving as a L_O,X_N type ligand.[36-38] This stands in contrast to the L_N,X_X coordination observed with classical products **Ni-3I** and **Ni-3Br**.

Comparing the ^{1}H NMR spectra of **Ni-3I**, **Ni-3Br**, and **[Ni-5]**$_2$ with that obtained following the reaction of **Ni-1** and **1** reveals a high degree of similarity with **[Ni-5]**$_2$, consistent with an analogous dimeric structure accounting for the persistent major product, (see above). This assignment suggests that dimerization of key oxidative addition intermediates introduces a thermodynamic trap, thereby accounting for the low TONs observed under catalytic conditions. Consistent with this hypothesis, [**Ni-5**]$_2$ is ineffective as a precatalyst, leading to no consumption of **1** under standard conditions.

Nonetheless, identification of the catalyst deactivation pathway informed strategies to overcome this limitation either by preventing dimerization or by providing a path for dimer dissociation (Scheme 5). Recognizing the bimolecular kinetic dependence of catalyst dimerization, we first assessed the impact of catalyst concentration on efficiency. However, neither decreasing the global concentration, nor reducing the loading of [**Ni-1**] resulted in any improvements to the catalyst TON or yield of biaryl **3** (Scheme 5B). Lewis basic additives were assessed with the goal of temporarily blocking the vacant coordination site in purported monomeric intermediate **Ni-5** (Scheme 5C).[39] Although slightly improved yields of **3** were observed upon addition of DMAP or potassium phthalimide (Kphth), the added Lewis bases were insufficient to overcome this challenge. Lewis acid additives were also evaluated, with the goal of promoting dissociation of [**Ni-5**]$_2$ through competitive coordination with the pyridonate O (Scheme 5D). However, neither ZnI_2 nor MgI_2 additives resulted in improved cross-coupling yields.

In summary, mechanistic study enabled identification of a unique catalyst deactivation pathway, involving ligand-promoted dimerization, in the context of a nickel-catalyzed Suzuki–Miyaura coupling. While additives proved to have limited beneficial effect in this case, the findings imply that polar electrophiles bearing more coordinating leaving groups may prove more effective for catalysis than their aryl or alkyl halide counterparts. Preliminary studies revealed that treatment of **Ni-1** with aryl phosphate esters, pivalates, or carbamates does not result in .[**Ni-5**]$_2$ formation. Ongoing work in our group is directed toward the use of these alternative electrophile classes in catalysis. Taken together, these results thus highlight challenges associated with ligand designs leveraging potentially reactive sites in the secondary coordination sphere, as well as potential solutions for these challenges.

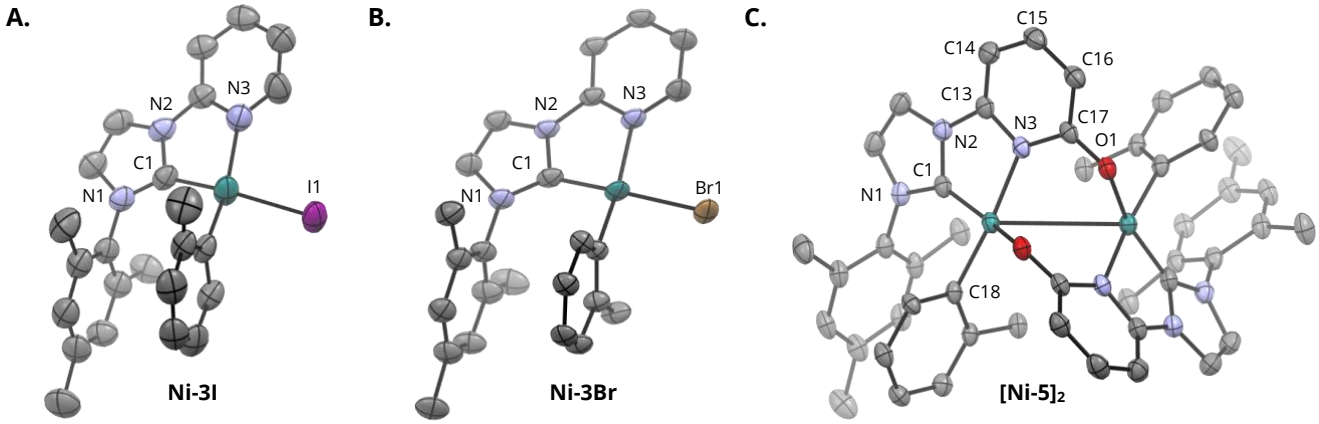

Figure 1. Solid-state structures of (A) **Ni-3I**, (B) **Ni-3Br**, and (C) **[Ni-5]$_2$** determined by single-crystal X-ray diffraction. Thermal ellipsoids depicted at 50% probability. H-atoms and co-crystallized solvent molecules omitted for clarity. Only one of two stereoisomers arising from disorder of the tolyl ligand over two positions shown for **Ni-3I** (0.54:0.46), **Ni-3Br** (0.62:0.38), and **[Ni-5]$_2$** (0.82:0.18). C = charcoal, N = blue, O = red, Ni = teal, Br = bronze, I = magenta

Table 1. Key metrics for the solid-state structures of Ni-3I, Ni-3Br, and [Ni-5]$_2$ determined by SC-XRD.

Bond lengths (Å) and dihedral angles (°)				Bond angles (°)			
	Ni-3I	**Ni-3Br**	**[Ni-5]$_2$**		**Ni-3I**	**Ni-3Br**	**[Ni-5]$_2$**
Ni(1)-X	2.503(5)	2.3341(6)	1.9187(16)	C(1)-Ni(1)-X	163.8(8)	168.39(9)	159.06(8)
	2.550(4)				169.0(7)		
Ni(1)-N(3)	2.016(6)	2.008(2)	1.9755(19)	C(1)-Ni(1)-N(3)	83.2(2)	82.63(11)	82.29(9)
	2.005(6)				82.4(3)		
Ni(1)-C(1)	1.845(6)	1.867(3)	1.857(2)	C(1)-Ni(1)-C(18)	94.1(8)	96.9(4)	95.39(10)
	1.891(7)				95.8(9)	91.2(6)	93.4(3)
Ni(1)-C(18)	1.911(8)	1.906(5)	1.910(3)	C(18)-Ni(1)-X	87.0(8)	88.5(4)	86.79(9)
	1.900(8)	1.914(7)	1.914(8)		90.5(9)	92.3(6)	98.4(3)
N(3)-C(13)	1.337(6)	1.340(4)	1.351(3)	C(18)-Ni(1)-N(3)	170.2(10)	166.3(3)	173.70(10)
N(3)-C(17)	1.344(7)	1.338(4)	1.359(3)		166.1(10)	172.7(6)	156.3(3)
C(13)-C(14)	1.380(6)	1.390(3)	1.364(3)	N(3)-Ni(1)-X	98.2(2)	94.50(8)	93.30(7)
C(14)-C(15)	1.379(7)	1.380(5)	1.401(4)		93.7(2)		
C(15)-C(16)	1.370(8)	1.377(5)	1.371(4)	N(1)-C(1)-N(2)	103.1(4)	102.9(2)	103.37(19)
C(16)-C(17)	1.377(8)	1.389(4)	1.423(3)	C(13)-N(3)-C(17)	116.6(4)	117.9(2)	119.00(19)
O(1)-C(17)	--	--	1.279(3)	N(3)-C(13)-C(14)	124.2(5)	123.9(3)	125.0(2)
				C(13)-C(14)-C(15)	117.7(5)	117.0(3)	116.1(2)
C(1)-N(2)-C(13)-N(3)	2.7(6)	1.1(4)	3.9(3)	C(14)-C(15)-C(16)	119.4(5)	120.1(3)	120.7(2)
C(1)-N(2)-C(13)-C(14)	-176.8(4)	-178.2(3)	-177.7(2)	C(15)-C(16)-C(17)	119.0(6)	118.9(3)	119.9(2)
				C(17)-O(1)–Ni(1')	--	--	125.65(14)
				N(3)-C(17)-O(1)	--	--	119.7(2)

EXPERIMENTAL SECTION

General Experimental Details. All air- and moisture-sensitive techniques were carried out using standard Schlenk technique on a high-vacuum line[40] or in an M. Braun glovebox containing an atmosphere of N_2. The glovebox was equipped with vacuum feed-throughs, a cold well, and a freezer for storing samples at –30 °C. Additional details are provided in the Supporting Information.

General Procedure for Catalytic Screening. In an N_2-filled glovebox, a 1-dram via equipped with a PTFE coated stir bar was charged with nickel complex **Ni-1** (0.014 g, 0.010 mmol, 10 mol %), 4-methoxyboronic acid (**2**, 0.061 g, 0.4 mmol, 2.0 equiv), additive (0.02–0.4 mmol, 0.2–2.0 equiv), then 4-fluoroiodobenzene (**1**, 23 μL, 0.2 mmol. 1.0 equiv) and solvent (1.0 mL). The vial was capped and sealed with electrical tape, removed from the glovebox, and stirred at 80 °C for 16 h. The vial was then opened to air, dodecane (20 μL) was added as an internal standard, and an aliquot was removed for gas chromatographic analysis. The crude reaction mixture was passed through silica and eluted with 7:3 hexanes/ethyl acetate (15 mL). The filtrate was concentrated in vacuo and then dissolved in $CDCl_3$ for analysis by ^{19}F and ^{1}H NMR spectroscopy using fluorobenzene and/or dibromomethane as internal standards, respectively.

Scheme 5. Hypothesis-driven modification of reaction conditions to overcome catalyst deactivation.

A.

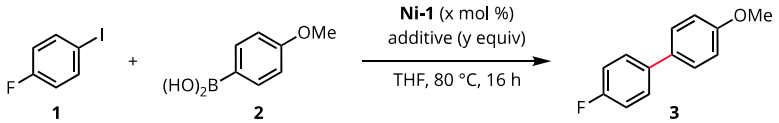

1 (1 equiv) **2** (2 equiv.) **3**

B.

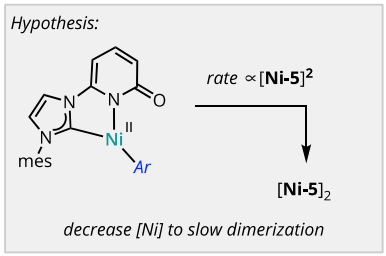

with no additive:

x	$[\mathbf{1}]_0$	Conv. of **1** [a]	Yield of **3** (TON) [b]
10	0.2 M	23%	6% (<1)
10	0.1 M	21%	5% (<1)
5	0.2 M	8%	2% (<1)

C.

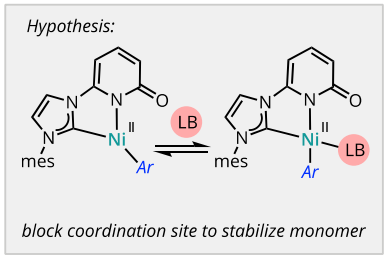

with 10 mol% **Ni-1** at $[\mathbf{1}]_0$ = 0.2 M:

Additive (equiv)	Conv. of **1** [a]	Yield of **3** (TON) [b]
DMAP (1.0)	18%	7% (<1)
Hphth (1.0)	20%	4% (<1)
Kphth(1.0)	12%	11% (~1)
Hphth (1.0) + KO^{t}Bu (2.0)	14%	4% (<1)

D.

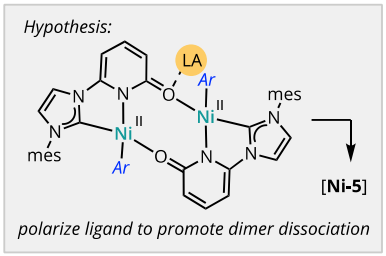

with 10 mol% **Ni-1** at $[\mathbf{1}]_0$ = 0.2 M:

Additive (equiv)	Conv. of **1** [a]	Yield of **3** (TON) [b]
ZnI_2 (1.0)	5%	3% (<1)
MgI_2 (1.0)	4%	4% (<1)

[a] Determined by gas chromatography from integration relative to dodecane as an internal standard. [b] Based on ^{1}H and ^{19}F NMR integration of diagnostic resonances relative to dodecane and fluorobenzene as internal standards.

ASSOCIATED CONTENT

Supporting Information

The Supporting Information is available free of charge on the ACS Publications website.

Experimental details, compound characterization data, and supplementary results (PDF)

Crystallographic data for **Ni-3I** (CCDC 2359151), **Ni-3Br** (CCDC 2359153), and **[Ni-5]$_2$** (CCDC 2359152) (CIF)

AUTHOR INFORMATION

Corresponding Author

C. Rose Kennedy — Department of Chemistry, University of Rochester, Rochester, New York 14627; orcid.org/0000-0003-3681-819X Email: c.r.kennedy@rochester.edu

Authors

Abhishek A. Kadam — Department of Chemistry, University of Rochester, Rochester, New York 14627; orcid.org/0000-0001-9453-2996

Medina Afandiyeva — Department of Chemistry, University of Rochester, Rochester, New York 14627; orcid.org/0000-0003-4454-5996

William W. Brennessel — Department of Chemistry, University of Rochester, Rochester, New York 14627; orcid.org/0000-0001-5461-1825

Notes

The authors declare no competing financial interest.

ACKNOWLEDGMENT

Financial support was provided by the University of Rochester. M.A. acknowledges the University of Rochester Elon Huntington-Hooker Award for fellowship support. Acquisition of JEOL 400 and 500 MHz NMR instruments (CHE-2215973) and a Rigaku XtaLAB Synergy-S Dualflex diffractometer (CHE-1725028) was enabled by funding from the National Science Foundation MRI program. The authors thank Ray Teng and Dr. Jason Holt (University of Rochester) for technical assistance and Dr. Tessa Baker (University of Rochester) for guidance with NMR spectroscopy.

REFERENCES

(1) Miyaura, N.; Suzuki, A. Palladium-Catalyzed Cross-Coupling Reactions of Organoboron Compounds. *Chem. Rev.* **1995**, *95* (7), 2457-2483. DOI: 10.1021/cr00039a007.

(2) Suzuki, A. Cross-Coupling Reactions Of Organoboranes: An Easy Way To Construct C–C Bonds (Nobel Lecture). *Angew. Chem. Int. Ed.* **2011**, *50* (30), 6722-6737. DOI: 10.1002/anie.201101379.

(3) Buskes, M. J.; Blanco, M. J. Impact of Cross-Coupling Reactions in Drug Discovery and Development. *Molecules* **2020**, *25* (15), 3493. DOI: 10.3390/molecules25153493.

(4) King, A. O.; Yasuda, N. Palladium-Catalyzed Cross-Coupling Reactions in the Synthesis of Pharmaceuticals. In *Organometallics in Process Chemistry*, Springer, 2004; pp 205-245.

(5) de Vries, J. G. Palladium-Catalysed Coupling Reactions. In *Organometallics as Catalysts in the Fine Chemical Industry*, Beller, M., Blaser, H.-U. Eds.; Springer, 2012; pp 1-34.

(6) Walters, W. P.; Green, J.; Weiss, J. R.; Murcko, M. A. What Do Medicinal Chemists Actually Make? A 50-Year Retrospective. *J. Med. Chem.* **2011**, *54* (19), 6405–6416. DOI: 10.1021/jm200504p.

(7) Bhutani, P.; Joshi, G.; Raja, N.; Bachhav, N.; Rajanna, P. K.; Bhutani, H.; Paul, A. T.; Kumar, R. U.S. FDA Approved Drugs from 2015–June 2020: A Perspective. *J. Med. Chem.* **2021**, *64* (5), 2339–2381. DOI: 10.1021/acs.jmedchem.0c01786.

(8) Blakemore, D. Suzuki–Miyaura Coupling. In *Synthetic Methods in Drug Discovery*, Vol. 1; The Royal Society of Chemistry, 2016; pp 1-69.

(9) Martin, R.; Buchwald, S. L. Palladium-Catalyzed Suzuki−Miyaura Cross-Coupling Reactions Employing Dialkylbiaryl Phosphine Ligands. *Acc. Chem. Res.* **2008**, *41* (11), 1461-1473. DOI: 10.1021/ar800036s.

(10) Li, H.; Johansson Seechurn, C. C. C.; Colacot, T. J. Development of Preformed Pd Catalysts for Cross-Coupling Reactions, Beyond the 2010 Nobel Prize. *ACS Catal* **2012**, *2* (6), 1147-1164. DOI: 10.1021/cs300082f.

(11) Lennox, A. J. J.; Lloyd-Jones, G. C. Transmetalation in the Suzuki–Miyaura Coupling: The Fork in the Trail. *Angew. Chem. Int. Ed.* **2013**, *52* (29), 7362-7370. DOI: 10.1002/anie.201301737.

(12) Amatore, C.; Le Duc, G.; Jutand, A. Mechanism of Palladium-Catalyzed Suzuki–Miyaura Reactions: Multiple and Antagonistic Roles of Anionic "Bases" and Their Countercations. *Chem. Eur. J.* **2013**, *19* (31), 10082-10093. DOI: 10.1002/chem.201300177.

(13) Tasker, S. Z.; Standley, E. A.; Jamison, T. F. Recent advances in homogeneous nickel catalysis. *Nature* **2014**, *509* (7500), 299-309. DOI: 10.1038/nature13274.

(14) Ananikov, V. P. Nickel: The "Spirited Horse" of Transition Metal Catalysis. *ACS Catal.* **2015**, *5* (3), 1964-1971. DOI: 10.1021/acscatal.5b00072.

(15) Han, F.-S. Transition-metal-catalyzed Suzuki–Miyaura cross-coupling reactions: a remarkable advance from palladium to nickel catalysts. *Chem. Soc. Rev.* **2013**, *42* (12), 5270-5298. DOI: 10.1039/C3CS35521G.

(16) Hazari, N.; Melvin, P. R.; Beromi, M. M. Well-defined nickel and palladium precatalysts for cross-coupling. *Nat. Rev. Chem.* **2017**, *1* (3), 0025. DOI: 10.1038/s41570-017-0025.

(17) Yamaguchi, J.; Muto, K.; Itami, K. Recent Progress in Nickel-Catalyzed Biaryl Coupling. *Eur. J. Org. Chem.* **2013**, *2013* (1), 19-30. DOI: 10.1002/ejoc.201200914.

(18) Partyka, D. V. Transmetalation of Unsaturated Carbon Nucleophiles from Boron-Containing Species to the Mid to Late d-Block Metals of Relevance to Catalytic C−X Coupling Reactions (X = C, F, N, O, Pb, S, Se, Te). *Chem. Rev.* **2011**, *111* (3), 1529-1595. DOI: 10.1021/cr1002276.

(19) Payard, P.-A.; Perego, L. A.; Ciofini, I.; Grimaud, L. Taming Nickel-Catalyzed Suzuki-Miyaura Coupling: A Mechanistic Focus on Boron-to-Nickel Transmetalation. *ACS Catal.* **2018**, *8* (6), 4812-4823. DOI: 10.1021/acscatal.8b00933.

(20) Christian, A. H.; Müller, P.; Monfette, S. Nickel Hydroxo Complexes as Intermediates in Nickel-Catalyzed Suzuki–Miyaura Cross-Coupling. *Organometallics* **2014**, *33* (9), 2134-2137. DOI: 10.1021/om5001327.

(21) Huheey, J. E.; Keiter, E. A.; Keiter, R. L. *Inorganic Chemistry: Principles of Structure and Reactivity, Fourth Edition*; Harper Collins, 1993.

(22) Hartwig, J. F. *Organotransition Metal Chemistry: From Bonding to Catalysis*; University Science Books, 2010.

(23) Afandiyeva, M.; Kadam, A. A.; Wu, X.; Brennessel, W. W.; Kennedy, C. R. Synthesis, Structure, and Hydroboration Reactivity of Anionic Nickel(0) Complexes Supported by Bidentate NHC-Pyridone Ligands. *Organometallics* **2022**, *41* (21), 3014-3023. DOI: 10.1021/acs.organomet.2c00439.

(24) Afandiyeva, M.; Wu, X.; Brennessel, W. W.; Kadam, A. A.; Kennedy, C. R. Secondary-sphere preorganization enables nickel-catalyzed nitrile hydroboration. *Chem. Commun.* **2023**, *59* (90), 13450-13453. DOI: 10.1039/D3CC04229D.

(25) Prakasham, A. P.; Ghosh, P. Nickel N-heterocyclic carbene complexes and their utility in homogeneous catalysis. *Inorg. Chim. Acta* **2015**, *431*, 61–100. DOI: 10.1016/j.ica.2014.11.005.

(26) Nett, A. J.; Cañellas, S.; Higuchi, Y.; Robo, M. T.; Kochkodan, J. M.; Haynes, M. T.; Kampf, J. W.; Montgomery, J. Stable, Well-Defined Nickel(0) Catalysts for Catalytic C–C and C–N Bond Formation. *ACS Catal.* **2018**, *8* (7), 6606–6611. DOI: 10.1021/acscatal.8b02187.

(27) Dander, J. E.; Garg, N. K. Breaking Amides using Nickel Catalysis. *ACS Catal.* **2017**, *7* (2), 1413–1423. DOI: 10.1021/acscatal.6b03277.

(28) Yang, J.; Neary, M. C.; Diao, T. ProPhos: A Ligand for Promoting Nickel-Catalyzed Suzuki-Miyaura Coupling Inspired by Mechanistic Insights into Transmetalation. *J. Am. Chem. Soc.* **2024**, *146* (9), 6360-6368. DOI: 10.1021/jacs.4c00370.

(29) Moss, J. R.; Shaw, B. L. Nuclear magnetic resonance studies on metal complexes. Part IV. Arylnickel(II)–dimethylphenylphosphine complexes. *J. Chem. Soc. A* **1966**, 1793-1795. DOI: 10.1039/J19660001793.

(30) Uchino, M.; Asagi, K.; Yamamoto, A.; Ikeda, S. Preparation and properties of aryl(dipyridyl)nickel halide complexes. *J. Organomet. Chem.* **1975**, *84* (1), 93-103. DOI: 10.1016/S0022-328X(00)88778-1.

(31) Shields, J. D.; Gray, E. E.; Doyle, A. G. A Modular, Air-Stable Nickel Precatalyst. *Org. Lett.* **2015**, *17* (9), 2166-2169. DOI: 10.1021/acs.orglett.5b00766.

(32) Standley, E. A.; Smith, S. J.; Müller, P.; Jamison, T. F. A Broadly Applicable Strategy for Entry into Homogeneous Nickel(0) Catalysts from Air-Stable Nickel(II) Complexes. *Organometallics* **2014**, *33* (8), 2012-2018. DOI: 10.1021/om500156q.

(33) Hidai, M.; Kashiwagi, T.; Ikeuchi, T.; Uchida, Y. Oxidative additions to nickel(0): preparation and properties of a new series of arylnickel(II) complexes. *J. Organomet. Chem.* **1971**, *30* (2), 279-282. DOI: 10.1016/S0022-328X(00)90208-0.

(34) Craig, S. M.; Malyk, K. R.; Silk, E. S.; Nakamura, D. T.; Brennessel, W. W.; Kennedy, C. R. Synthesis and characterization of Ni(0) complexes supported by an unsymmetric C,N ligand. *J. Coord. Chem.* **2022**, *75* (11-14), 1841-1852. DOI: 10.1080/00958972.2022.2117037.

(35) Bajo, S.; Laidlaw, G.; Kennedy, A. R.; Sproules, S.; Nelson, D. J. Oxidative Addition of Aryl Electrophiles to a Prototypical Nickel(0) Complex: Mechanism and Structure/Reactivity Relationships. *Organometallics* **2017**, *36* (8), 1662-1672. DOI: 10.1021/acs.organomet.7b00208.

(36) Hejazi, S. A.; Osman, O. I.; Alyoubi, A. O.; Aziz, S. G.; Hilal, R. H. The Thermodynamic and Kinetic Properties of 2-Hydroxypyridine/2-Pyridone Tautomerization: A Theoretical and Computational Revisit. *Int. J. Mol. Sci.* **2016**, *17* (11), 1893. DOI: 10.3390/ijms17111893.

(37) Wong, M. W.; Wiberg, K. B.; Frisch, M. J. Solvent effects. 3. Tautomeric equilibria of formamide and 2-pyridone in the gas phase and solution: an ab initio SCRF study. *J. Am. Chem. Soc.* **2002**, *114* (5), 1645–1652. DOI: 10.1021/ja00031a017.

(38) Rawson, J. M.; Winpenny, R. E. P. The coordination chemistry of 2-pyridone and its derivatives. *Coord. Chem. Rev.* **1995**, *139*, 313–374. DOI: 10.1016/0010-8545(94)01117-T.

(39) Prieto Kullmer, C. N.; Kautzky, J. A.; Krska, S. W.; Nowak, T.; Dreher, S. D.; MacMillan, D. W. C. Accelerating reaction generality and mechanistic insight through additive mapping. *Science* **2022**, *376* (6592), 532-539. DOI: 10.1126/science.abn1885.

(40) Burger, B. J.; Bercaw, J. E. Vacuum Line Techniques for Handling Air-Sensitive Organometallic Compounds. In *Experimental Organometallic Chemistry*, ACS Symposium Series, Vol. 357; American Chemical Society, 1987; pp 79–115.